RSC Advances

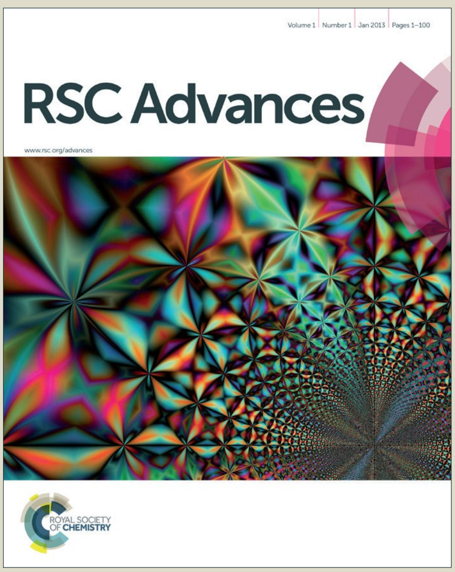

Role of inorganic ions and dissolved natural organic matters on persulfate oxidation of acid orange 7 with zero-valent iron

Huanxuan Li[a, b], Jinquan Wan[a, b, c, *], Yongwen Ma[a, b, c], Yan Wang[a, b], Zeyu Guan[a,b]

[a] School of Environment and Energy, South China University of Technology, Guangzhou 510006, PR China

[b] The Key Lab of Pollution Control and Ecosystem Restoration in Industry Clusters, Ministry of Education, China, Guangzhou 510006, PR China

[c] State Key Lab Pulp and Paper Engineering, South China University of Technology, Guangzhou 510640, PR China

Corresponding author at: School of Environment and Energy, South China University of Technology, Guangzhou 510006, China. E-mail address: ppjqwan@scut.edu.cn (J. Wan).

Tel.: +86 20 87114970, Fax: +86 20 39380560

Abstract:

The impacts of common anions and organic matters, initial pH and PS dosage on the oxidation of acid orange 7 (AO7) by persulfate (PS) activated with zero-valent iron (ZVI) were investigated. The present findings revealed that maximum AO7 decolorization occurred at pH 3.0, increasing system pH resulted in a greater decrease in AO7 decolorization rates. AO7 decolorization efficiency was 100% at 120 min when the molar ratio of PS:AO7 was 5:1. Interestingly, ClO_4^-, CH_3COO^- and humic acid (HA) were found to accelerate AO7 decolorization rates while other anions retarded AO7 decolorization in the following sequence: NO_2^- > $H_2PO_4^-$ > HPO_4^{2-} > EDTA > SO_4^{2-} > CO_3^{2-} > HCO_3^- > NO_3^-> Cl^-. ClO_4^-, CH_3COO^- and HA with 50 mM, 10 mM and 1.0 mg/L, respectively were found to be the optimal concentrations for AO7 decolorization. The removal efficiencies of AO7 were decreased by 90.3%, 51.5%, 58.7% and 38.2%, respectively over 120 min in addition of NO_2^- (50 mM), $H_2PO_4^-$ (50 mM), HPO_4^{2-} (50 mM) and EDTA (50 mM). The other anions including SO_4^{2-}, CO_3^{2-}, HCO_3^-, NO_3^- and Cl^- led to a decrease change of less than 20%. The mechanisms for the influence were complexation reactions with Fe^{2+} generated from ZVI, consuming of sulfate radicals ($SO_4^{-\bullet}$) by scavenging reactions, and oxidation reactions involving inorganic ions. The reason for the acceleration by CH_3COO^- and HA was probably through acting as an electron 'shuttle' and facilitating electron transfer from ZVI surface to PS and resulted in more Fe^{2+} and $SO_4^{-\bullet}$. However, the acceleration caused by ClO_4^- was presumably ascribed to the oxidizing of ZVI directly by ClO_4^- to produce more Fe^{2+}.

Keywords: Persulfate (PS), Zero-valent iron (ZVI), Acid orange 7(AO7), Inorganic ions, Organic matters

1. Introduction

Synthetic dyes have received increasing attention in recent years due to their wide use in many industries such as textile, cosmetic, pulp and paper[1]. As one of the most widely used synthetic dyes, azo dyes are ubiquitous in environments[2] because of their high solubility in water, which would cause harm to aquatic organisms and human health due to their toxic and potential carcinogenic nature[1]. Another potential disadvantage is from the fact that azo dyes are difficult to degrade by biological treatment methods due to their complex structure and stability[3].

Advanced oxidation processes (AOPs) involve the generation of free radicals, notably hydroxyl radicals ($HO^{\bullet}$) and sulfate radicals ($SO_4^{-\bullet}$) that are highly oxidative and capable of degrading a wide range of organic compounds[4]. Typical AOP was based on the generation of $HO^{\bullet}$, such as the Fenton reaction[5]. Recently, AOP that generates nonselective $SO_4^{-\bullet}$ by activation of persulfate ion

($S_2O_8^{2-}$, PS)[6] or peroxymonosulfate (PMS)[7] has attracted a great deal of interest. Compared to the Fenton reagent and other oxidants, some properties of PS including high aqueous solubility, more chemically stable in subsurface, relatively low cost, easy storage and transport make it to be a promising oxidant of in-situ chemical oxidation (ISCO) which is a technique used to remediate contaminated soil and groundwater systems[6]. $SO_4^{-\bullet}$ has a high oxidizing potential of 2.5-3.1 versus normal hydrogen electrode (NHE)[6], which makes it an excellent oxidant for degrading a wide range of recalcitrant and/or toxic organic pollutants in water and soil[8-10]. Generally, $SO_4^{-\bullet}$ can be produced from the activation of PS by UV[8,9], heat[10], and transition metal ions[11-13].

Photochemical activation: $S_2O_8^{2-} + hv^{-} \rightarrow 2SO_4^{-\bullet}$ (1)

Thermal activation: $S_2O_8^{2-} + heat \rightarrow 2SO_4^{-\bullet}$ (2)

Chemical activation: $S_2O_8^{2-} + M^{n+} \rightarrow SO_4^{-\bullet} + M^{(n+1)+} + SO_4^{2-}$ (3)

Among the various activation methods, zero-valent iron (ZVI) activation of PS has appeared to be a promising method[14-16]. ZVI activation is a cost-effective, efficient and environmentally friendly technology[14,17]. Additionally, ZVI not only serves as a slow-releasing source of dissolved Fe^{2+}, but also avoids adding other anions that can lead to scavenging of $SO_4^{-\bullet}$ and possibly reducing the oxidation efficiency[18,19]. Because the competing side reactions of $SO_4^{-\bullet}$ with these anions rather than the target pollutant would occur.

Recently, one of the limitation factors in the use of PS for degradation of organic pollutants is the reactions between the produced radicals and nontarget chemical species that are naturally occurring or anthropogenic present in the wastewater[19,20]. Besides the refractory contaminants, waster waters usually contain a certain amount of other substances such as inorganic ions and common dissolved natural organic matters. It was reported that the concentrations levels of sulfate and chloride anions in groundwater vary from 0.1 to 100 mM[21]. Other naturally abundant inorganic anions such as nitrate, carbonate and phosphate anions are frequently present in water, wastewater or seawater with various concentrations. The existence of these substances may affect the degradation rate of target contaminant by serving as proton donors, electron shuttles, or competing for electrons, and thereby affecting the oxidation efficiency of the target pollutant[22]. Also, common organic matters and anions have the potential to impact pathway and kinetic of oxidation reactions both as radical scavengers and metal complexing agents[21,23]. This may result in limiting the reactivity of $SO_4^{-\bullet}$ by the presence of background ions in wastewaters. Based on Liang's research, the Cl^- would exhibit an inhibition effect on the degradation of TCE by thermal/PS once the concentration of Cl^- was greater than 0.2 mM[24]. Carbonates also reduced the decomposition rates of contaminant and oxidant in the PS oxidation system[25]. While effects of anions on heat, UV light and ferrous ion activation methods have been studied[26,27], literature of anions on the behavior of ZVI activating of PS is very limited. Recently, we have reported influence of particle size of ZVI and dissolved silica on the reactivity of activating PS for degradation of AO7[26]. However, the effects of other common organic matters and anions on the decolorization of AO7 are also needed to understand. Moreover, in the research of influence of anions in the PS systems, researchers did not deeply study the retardation or promoting mechanisms. Therefore, in the present study we aim to better understand the behavior of the common anions and organic matters on the $SO_4^{-\bullet}$-based treatment of organic contaminants, using PS/ZVI/AO7 as a model AOP treatment technology. Therefore, the objective of this research is to gain insight into: (1) the influence of both acidity anions and alkalinity anions on the removal of AO7 in the PS/ZVI system, (2) the impacts of dissolved natural organic matters on the decomposition of AO7 and PS, (3) the influence mechanism of these common organic matters and anions.

2. Materials and methods

2.1 Materials

The ZVI (purity > 99%, approx. 150μm), humic acid (HA, fulvic acid (FA) ⩾ 90%), and sodium perchlorate ($NaClO_4$, 99.0%) were obtained from Aladdin chemistry Co., Ltd (Shanghai, China). The total surface area (α_s) of ZVI was 2.1518 m^2g^{-1} according to the N_2 isothermal adsorption. AO7 (purity > 99.0%) was purchased from Tokyo Chemical Industry (Japan). Sodium persulfate (PS, $Na_2S_2O_8$, 98.0%), sodium chloride (NaCl, 99.5%), sodium sulfate (Na_2SO_4, 99.0%), sodium bicarbonate ($NaHCO_3$, 99.5%), sodium carbonate (Na_2CO_3, 99.0%), sodium phosphate dibasic trihydrate ($Na_2HPO_4 \cdot 3H_2O$, 99.0%), sodium nitrate ($NaNO_3$, 99.0%), sodium nitrite ($NaNO_2$, 99.0%), ethylene diamine tetraacetic acid disodium (EDTA-2Na, 98.0%), potassium iodide (KI, 99.0%), and other chemicals used were purchased from Sinopharm Chemical Reagent Co., Ltd (Beijing, China). All chemicals were used as received without any further purification.

2.2 Experimental procedure

The experimental setup was similar to our previously study[15]. Reactions were carried out in a 250-mL Erlenmeyerl flask at 25 ± 0.2 ℃. Fifty millilitres of the prepared AO7 (0.4 mM) and PS (4 mM) stock solutions were added simultaneously to the reactor, giving initial concentrations of AO7 and PS of 0.2 mM and 2.0 mM, respectively. Reaction mixtures in the flask were subsequently added 0.5 mL of inorganic ions or organic matters stock solution with high concentration. The flask was open to the atmosphere and shaken at 180 rpm in a rotary shaker (ZHWY-20102C, Shanghai, China). All reactions were initiated by adding ZVI, then samples were withdrawn in the predetermined time intervals, and then a certain amount of ethanol (1.0 mL of ethanol for each 1.0 mL sample) was added to quench the reaction[28]. The supernatant was filtered through a 0.45-μm membrane filter and analyzed for AO7, PS, Fe^{2+} and total dissolved iron. In order to avoid potential complications by buffers or ionic strength, all experiments except the effect of initial pH were performed without pH adjustment and to give initial pHs of 3.8. But the pHs varied dramatically after adding inorganic anions or organic matters, the pH of reaction solutions containing inorganic anions or organic matters was displayed in Tables S1 and S2. In the experiment of effect of initial pH, the initial pH value was adjusted with 1.0 M sodium hydroxide (NaOH) or sulfuric acid (H_2SO_4).

2.3 Analytical methods

The absorbance of Acid Orange 7 was measured in visible spectra at the characteristic wavelength of AO7 (λ_{max} = 486 nm) using a UV-Vis spectrophotometer (UV2301 II, Shanghai, China). Decolorization efficiency (η) was calculated based on the following equation: $\eta\ (\%) = (A_0\text{-}A)/A_0 \times 100$, where the A_0 and A were the absorbance of the sample at time 0 and t, respectively. The PS residual was determined by spectrophotometric determination with potassium iodide[29], and the concentrations of ferrous iron and dissolved iron were measured with 1, 10-phenanthroline at a wavelength of 510 nm[30]. The concentrations of some anions were measured by ion chromatography (DX 500, USA). The pH was monitored by pH meter (Shanghai LeiCi PHS-25) equipped with a pH electrode.

3. Results and discussion

3.1 Effect of initial pH and PS dosage

The pH value of aqueous solution plays an important role in the degradation of organic compounds in the advance oxidation processes. To confirm the effect of initial pH on the decolorization rate of AO7, a series of experiments were carried out with initial pH values ranging from 3.0 to 11.0 (seen in Fig. 1). Clearly, AO7 could completely decolor over a wide pH range of 3.0-9.0. Moreover, the solution pH significantly influenced the AO7 decolorization rates, which decreased with the increase of the initial pH values. It can be derived from this result that the acidic solution was more favorable than neutral and alkaline solutions for generating of $SO_4^{-\bullet}$. The AO7 decolorization under different initial pH was observed to fit the pseudo-first order kinetic model well ($[AO7]/[AO7]_0 = \exp(-k_{obs}\, t)$) with a correlation coefficient R^2 value greater than 0.96, where the k_{obs} represented the pseudo-first-order rate constant. It can be seen (seen in Fig. 1b) that the rate constants decreased significantly when the pH increased from 3.0 to 5.0. However, the AO7 decolorization rate constants showed small extent decrease while the solution pH values increased from 5.0 to 9.0.

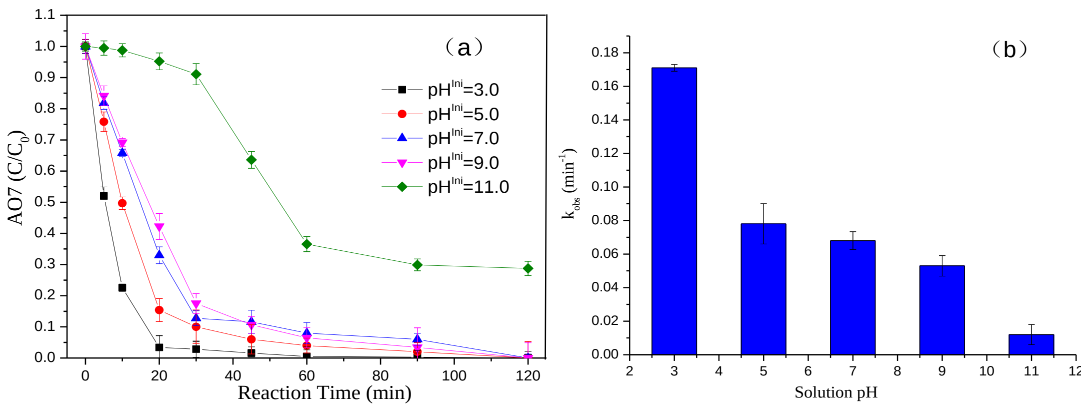

Fig.1. (a) The decolorization of AO7 under different initial pH values; (b) Pseudo-first-order rate constants of AO7 versus initial pH values. Experiment condition: PS = 2 mM; AO7 = 0.2 mM; ZVI = 0.5 g/L; T = 25 °C.

PS can be decomposed to produce $SO_4^{-\bullet}$ with the activation of catalysts, which makes a dominant contribution to removing organic contaminants. The influence of the molar ratios of PS to AO7 on the AO7 decolorization was studied. As illustrated in the Fig. 2, the concentrations of

PS appeared to be one of the crucial factors affecting the AO7 decolorization. The AO7 decolorization efficiency was noticeable higher at the molar ratio (PS:AO7) of 5:1 than that of 1:1. AO7 was decolorized completely in 120 min when the molar ratio of PS:AO7 exceed 5:1.

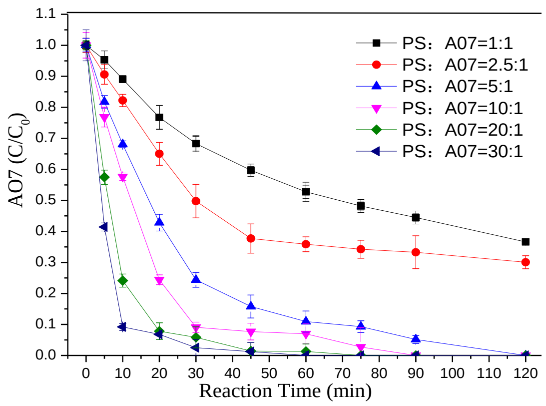

Fig. 2. The effect of PS dosage on the decolorization of AO7 versus reaction time. Experiment condition: AO7 = 0.2 mM; ZVI = 0.5 g/L; initial pH = 3.8 ± 0.1; T = 25 °C.

3.2 The role of common acidity anions

Usually, a great amount of dissolved inorganic ions may be present initially in the wastewater or formed as end products from the compounds undergoing degradation. Therefore, in order to clear the role of common acidity anions on the degradation of organic pollutants in the ZVI/PS system, the decolorization rate of AO7 was measured in the presence of acidity anions with the concentration of 50 mM. As shown in Fig. 3, it can be obviously found that the addition of different acidity inorganic ions led to different impact on decolorization of AO7 with ZVI activation of PS.

3.2.1 Nitrite and nitrate ions

Nitrite ion (NO_2^-) exhibited relatively deceleration on the decolorization of AO7, only about 10% of the AO7 was removed from solution over 120 min while the AO7 decolorization rate was 100% without NO_2^- under the identical conditions. However, it was interesting to note that the addition of nitrate ion (NO_3^-) showed a much smaller extent deceleration on the AO7 decolorization, whereas the AO7 decolorization efficiency were 90.0% and 94.3% within 60 min in the presence and absence of NO_3^-, respectively. In fact, ZVI has been known to reduce nitrate to nitrite, nitrogen, ammonium and ammonia depending upon experimental conditions, as well as zero valent aluminum and zero valent magnesium[31]. Moreover, NO_3^- does not complex with Fe^{3+} or Fe^{2+} measurably, nor does it react with hydroxide radical[32]. From which we can infer that the little inhibitory effect of NO_3^- may be ascribed to that NO_3^- competed with PS on electrons generated from ZVI corrosion. The deceleration decolorization caused by NO_3^- also confirmed the hypothesized mechanism of heterogeneous activation of PS, involving direct electron transfer from ZVI (see Eq. (4)).

$$Fe^0 + 2S_2O_8^{2-} \rightarrow Fe^{2+} + 2SO_4^{2-} + 2SO_4^{-\bullet} \qquad (4)$$

The remarkable effect of NO_2^- on the decolorization of AO7 was due to the transformation of NO_2^- to NO_3^- (see Eq. (5)), which consumed large amounts of $SO_4^{-\bullet}$ and caused the final pH lower than initial pH.

$$2SO_4^{-\bullet} + H_2O + NO_2^- \rightarrow NO_3^- + 2SO_4^{2-} + 2H^+ \qquad (5)$$

For NO_3^- was detected and increased when the NO_2^- concentration decreased during the reaction (data not shown). On the other hand, although the PS decomposition was also retarded in the presence of NO_2^- (Fig. 3b), the retardation effect was smaller than that of AO7. Based on these results, we speculated that the scavenging of $SO_4^{-\bullet}$ by NO_2^- was not mainly resulted in the deceleration effect. It was likely, however, the retardation effect on the decomposition of PS, which caused the low concentration of $SO_4^{-\bullet}$. Further experiments were conducted in various concentrations of NO_2^-. As shown in Table S3, the pseudo-first-order rate constants (k_{obs}) of the decolorization of AO7 in contact with NO_2^- concentrations ranging from 0 to 100.0 mM were obtained. The oxidation of AO7 exhibited great decrease in the rate constants from 0.048 min^{-1} to 0.001 min^{-1} with NO_2^- concentration increase from 0 to 50.0 mM. However, when the concentration of NO_2^- exceeded 50.0 mM, the k_{obs} increased to 0.002 min^{-1} and the half-life decreased correspondingly.

3.2.2 Sulfate ion

Evidently, the retention on the oxidation of AO7 was observed when the sulfate ion (SO_4^{2-}) was added into the PS/ZVI system (seen in Fig. 3a) even though they were poor free radical scavengers[33]. This effect was also reflected in the PS decomposition. However, compared to the control system without any anion, the presence of SO_4^{2-} led to a decrease of 52% change in decomposition of PS (seen in Fig. 3b) and only 14% change in decolorization of AO7 (seen in Fig. 3a). This verified that the retardation effect on decolorization of AO7 was not ascribed to scavenging of $SO_4^{-\bullet}$ by SO_4^{2-}. In contrast, the appearance of SO_4^{2-} made $SO_4^{-\bullet}$ more efficiently towards oxidation of AO7. This result can be attributed to the fact that SO_4^{2-} underwent complex reactions with Fe^{3+} and Fe^{2+} and formed a mixture of $FeSO_4^+$ and $Fe(SO_4)_2^-$ complexes, which decreased the concentration of Fe^{2+} and reduced Fe^{3+} through coordination[9]. In addition, it has been reported[34] that the presence of SO_4^{2-} could reduce oxygenation of Fe^{2+} in neutral and slightly acidic solution because of the formation of ion pairs ($FeSO_4$) that are more difficult to oxidize. Therefore, it was likely that the retardation effect caused by SO_4^{2-} could be overcome by extending the reaction time in this system.

3.2.3 Chloride and perchlorate ions

Based on research results of Liang et al.[23], there was hardly any interference emerging in the

TCE degradation with chloride levels below 0.2 M on PS oxidation of TCE at 20℃. Another study[20] showed that iron activation at neutral pH was not affected significantly by Cl^- with concentrations of 5.0 and 50.0 mM. In this study, the Cl^- and ClO_4^- revealed little effect both on the AO7 decolorization and PS decomposition (Fig. 3a). Compared to the AO7 decolorization, the presence of Cl^- resulted in a greater degree of retardation on the PS decomposition. These findings illustrated that the deceleration was attributed to the effective scavenging of $SO_4^{-\bullet}$ through the reactions (see Eq. (6) and (7))[35] of Cl^- with $SO_4^{-\bullet}$ generated from PS activated by ZVI.

$$SO_4^{-\bullet} + Cl^- \rightarrow SO_4^{2-} + Cl^{\bullet} \quad (6)$$

$$Cl^{\bullet} + Cl^- \rightarrow Cl_2^{-\bullet} \quad (7)$$

Perchlorate ions (ClO_4^-) are similar to NO_3^-, they do not react with Fe^{3+} or Fe^{2+} through complex reaction, nor do they react with free radicals. In the presence of ClO_4^-, Fe(II) exists as Fe^{2+} and $Fe(OH)^+$ at pH<8[36]. Hence, the reaction between Fe^{2+} and PS was not suppressed. However, it was interesting to find that pseudo-first-order rate constants for PS oxidation of AO7 increased from 0.048 min^{-1} to 0.074 min^{-1} (seen in Table S4) when the ClO_4^- concentration increased from 0 to 50.0 mM. This indicated that the AO7 decolorization was drastically enhanced by ClO_4^-. That was due to a probable reaction between ZVI and ClO_4^- (see Eq. (8)). The final pH was a little higher than the initial pH of PS+AO7+ZVI+ClO_4Na system also supported this conclusion. Because the final pH was usually lower than initial pH in $SO_4^{-\bullet}$-based AOPs[14,15]. Once the ClO_4^- concentrations exceed 50.0 mM, the rate constants decreased but they were still higher than the rate constant without ClO_4^-.

$$ClO_4^- + 4Fe^0 + 8H^+ \rightarrow 4Fe^{2+} + Cl^- + 4H_2O \quad (8)$$

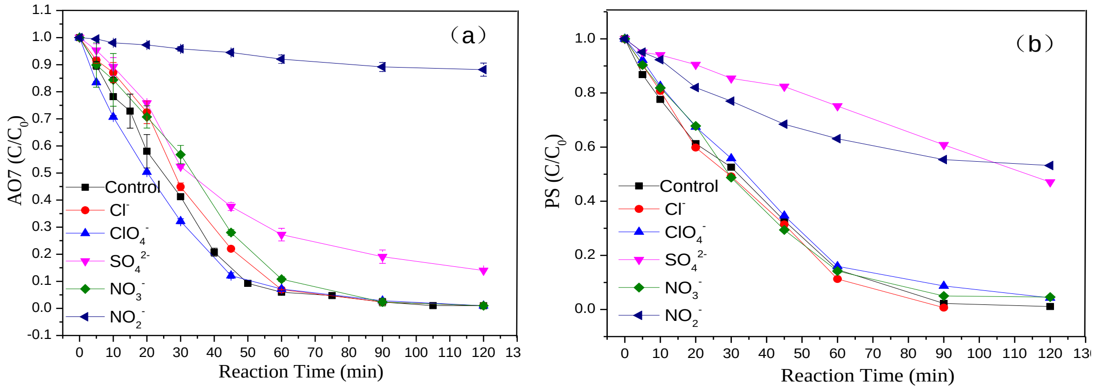

Fig. 3. (a). The effect of common acidity anions on the decolorization of AO7; (b). The effect of common acidity anions on the decomposition of PS. Experiment condition: PS = 2 mM; AO7 = 0.2 mM; ZVI = 0.5 g/L; Cl^- = 50 mM; ClO_4^- = 50 mM; SO_4^{2-} = 50 mM; NO_3^- = 50 mM; NO_2^- = 50 mM; T = 25 °C.

3.3 The role of common alkalinity anions

As evidence, the negativity of common alkalinity anions was greater than that of common acidity anions on the decolorization efficiency of AO7, which was showed in the Fig. 4.

3.3.1 Carbonates and bicarbonate ions

Carbonates ion (CO_3^{2-}) and bicarbonate ion (HCO_3^-) are well known buffer ions and often adopted to adjust the pH values, implying that they are expected to be extremely important species. It was reported that addition of CO_3^{2-} and HCO_3^- increased oxidation of Fe^{2+} forms dramatically, which was believed that this effect was due to the higher reactivity of $FeCO_3$ (than Fe^{2+} or $FeOH^+$) towards H_2O_2[37]. Furthermore, CO_3^{2-} are also believed to adsorb and inactivate catalytic and scavenging sites such as iron oxides[38]. As displayed in Fig. 4a, the PS reaction was extremely sensitive to CO_3^{2-} remaining in the solution, but the addition of HCO_3^- inhibited the AO7 decolorization to a much smaller extent. After 120 min of the reaction with PS, AO7 was decolorized in 96.2% in the presence of HCO_3^-. When CO_3^{2-} was introduced into the reaction solution, the amount of decolorized AO7 fell to 89.1%. The greater scavenging capacity of CO_3^{2-} >

HCO_3^- was considered to be the major reason responsible for this phenomenon. The rate constant for the reaction of $SO_4^{-\bullet}$ with HCO_3^- is about 4 times lower than that of $SO_4^{-\bullet}$ with CO_3^{2-} (see Eq. (9) and (10)). Moreover, the redox potential of $CO_3^{-}\bullet$ is lower than that of $HCO_3^{\bullet}$[39]. Accordingly, the inhibition impact on oxidation of AO7 by CO_3^{2-} was more pronounced than that of HCO_3^-. The $HCO_3\bullet$ and $CO_3^{-}\bullet$ generated by the reaction of $SO_4^{-\bullet}$ with HCO_3^- and CO_3^{2-} were reported to yield redox potential[23], which can possibly destroy AO7. But the generating rate and the redox potential of these two free radicals were significantly lower compared to $SO_4^{-\bullet}$, this revealed that the contribution of $HCO_3\bullet$ and $CO_3^{-}\bullet$ towards the oxidation of AO7 might be negligible.

$$SO_4^{-\bullet} + CO_3^{2-} \rightarrow SO_4^{2-} + CO_3^{-\bullet} \qquad (9)$$

$$SO_4^{-\bullet} + HCO_3^{-} \rightarrow SO_4^{2-} + HCO_3^{\bullet} \qquad (10)$$

3.3.2 Hydrogen phosphate and dihydrogen phosphate ions

The addition of hydrogen phosphate ion (HPO_4^{2-}) and dihydrogen phosphate ion ($H_2PO_4^-$) showed retardation effects on the decolorization of AO7, but the delay was more pronounced in the case of $H_2PO_4^-$. The removal efficiencies of AO7 in the presence of $H_2PO_4^-$ and HPO_4^{2-} were decreased by 51.5% and 58.7%, respectively. The markedly decreasing rates on decomposition of PS caused by $H_2PO_4^-$ were resulted from the complex compounds of $H_2PO_4^-$ with Fe^{2+} or Fe^{3+} (see Eq. (11) and (12)). These phosphate complexes are quite insoluble in neutral or mildly acidic solution.

$$Fe^{2+} + H_2PO_4^- \rightarrow FeH_2PO_4^+ \qquad (11)$$

$$Fe^{3+} + H_2PO_4^- \rightarrow FeH_2PO_4^{2+} \qquad (12)$$

Accordingly, precipitation of Fe (III) phosphate complexes presumably reduced the reactivity species of Fe^{2+} towards activating of PS. The inhibiting effect of $H_2PO_4^-$ on the rates of conversion of AO7 not only depended on the complexation of ferrous ions, but also resulted from competition with AO7 for $SO_4^{-\bullet}$ because $H_2PO_4^-$ reacted with $SO_4^{-\bullet}$ to generate inorganic radicals (see Eq. (13)).

$$SO_4^{-\bullet} + H_2PO_4^- \rightarrow H_2PO_4^{\bullet} + SO_4^{2-} \qquad (13)$$

$H_2PO_4^{\bullet}$, one of the strong oxidant species, react with most of the organic solutes with a high second-order rate constants that range from 10^6 to 10^9 M^{-1} s^{-1}, but they are still less reactive than $SO_4^{-\bullet}$. In the case of HPO_4^{2-}, it is well known that HPO_4^{2-} are efficient scavengers of HO•[34], maybe scavengers of $SO_4^{-\bullet}$ as well (see Eq. (14)). This hypothesis can be verified by the

$$SO_4^{-\bullet} + HPO_4^{2-} \rightarrow HPO_4^{-\bullet} + SO_4^{2-} \qquad (14)$$

decomposition of PS, which showed less extent inhibition effect than that of AO7. Apparently, the inhibition differences between these two phosphate ions were attributed to the phosphate complexes of iron.

3.3.3 Acetate ion

The effect of acetate ion (CH_3COO^-) on the decolorization of AO7 in PS/ZVI process was investigated (Fig. 4). Surprisingly, the decolorization rate underwent significant enhancement in the presence of 50.0 mM CH_3COO^- as compared to the control system with no added CH_3COO^-. In contrast, the concentration of remaining PS with CH_3COO^- was greater than that of the control system. This indicated that CH_3COO^- behaved differently from other common alkalinity anions, which not only increased the AO7 decolorization rate but also decreased the scavenging reactions that competed with AO7 for $SO_4^{-\bullet}$. Further study on the various concentration of CH_3COO^- were conducted, data presented in Table S5. It can be observed that increasing the concentrations of CH_3COO^- from 0 to 10.0 mM resulted in an increase in rate constants from 0.048 to 0.064 min^{-1}.

However, further increase of the CH_3COO^- concentrations beyond 10.0 mM led to gradual decrease in the rate constants. The concentrations of Fe^{2+}, total dissolved iron, and CH_3COO^- were monitored (Fig. 5) during the reaction in order to verify the influence mechanism. Observation of the concentration of Fe^{2+}, total dissolved iron indicated that the presence of CH_3COO^- could promote the release of Fe^{2+}, which was one of the main species that can activate PS to produce $SO_4^{-\bullet}$. Therefore, it was speculated that CH_3COO^- acted as an electron shuttle to promote the electron transfer from ZVI, and generate Fe^{2+} in this oxidation process. However, the speed of Fe^{2+} release was dramatically different from that of PS/Fe^{2+} system where supplied abundant Fe^{2+} instantaneously and resulted in a great amount of Fe^{2+} inactivating and declining AO7 and PS decomposition rate eventually, as shown in Fig. S1. The results demonstrated that the slow release of Fe^{2+} from ZVI was better than the direct addition of Fe^{2+}. It should be noted that the concentrations of CH_3COO^- decreased from 50 to 47.3 mM within 120 min, it was likely due to the formation of $^{\cdot}CH_2COO^-$ radical by H-abstraction reaction (see Eq. (15)). This also potentially explained why the final pH was much lower than the initial pH in the PS+AO 7+ZVI+CH_3COONa system.

$$SO_4^{-\bullet} + CH_3COO^- \rightarrow CH_2COO^{-}\cdot + SO_4^{2-} + H^+ \qquad (15)$$

This scavenging reaction caused the AO7 decolorization rate constant decreasing when the CH_3COO^- concentrations increased. Another mechanism for the enhancement effect might be the complex reactions. The reaction solution was clear all the time in the presence of CH_3COO^- while the solution gradually became turbid in the absence of CH_3COO^- because of the precipitation of Fe (III). This phenomenon helped to get the conclusion of complex reactions in the absence of CH_3COO^-.

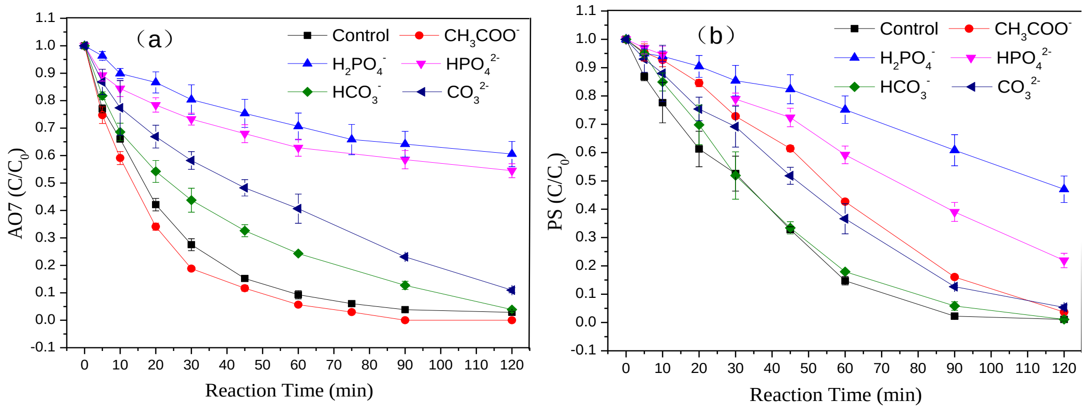

Fig. 4. (a). The effect of alkalinity anions on the decolorization of AO7 versus reaction time; (b). The effect of alkalinity anions on the decomposition of PS versus reaction time. Experiment condition: PS = 2 mM; AO7 = 0.2 mM; ZVI = 0.5 g/L; CO_3^{2-} = 50 mM; HCO_3^- = 50 mM; HPO_4^{2-} = 50 mM; $H_2PO_4^-$ = 50 mM; CH_3COO^- = 50 mM; T = 25 °C.

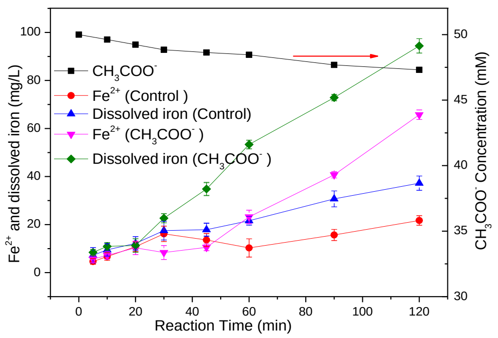

Fig. 5. The variation of iron ions in the presence and absence of CH_3COO^- versus reaction time. Experiment condition: PS = 2 mM; AO7 = 0.2 mM; CH_3COO^- = 50 mM; ZVI = 0.5 g/L; T = 25 °C.

3.4 The role of common organic matters

3.4.1 Ethylene diamine tetraacetic acid

As one of the most widely used chelating agents, ethylene diamine tetraacetic acid (EDTA) is routinely used to remove heavy metal ions from hard water or in industrial cleaning[40]. More recently, EDTA was adopted as chelating agents to improve the treatment efficiency by slow releasing Fe^{2+} in AOPs[41,42]. Therefore, the impact of EDTA on the degradation of organic pollutant seems to be important in AOPs. It was seen (seen in Fig.6) that both AO7 and PS decomposition were retarded in the presence of 50 mM EDTA. The control system with PS but no ZVI, AO7 and PS were almost not decomposed, which revealed that EDTA showed little influence on the activation of PS. Consequently, this was speculated that retardation effect was due to chelating Fe^{2+} by EDTA. On the other hand, oxidation of EDTA by $SO_4^{-\bullet}$ also resulted in AO7 decolorization decrease.

3.4.2 Humic acid

Humic acid (HA) is one of the important component of natural systems, the role of HA on the PS oxidation reaction has not been reported, to the best of our knowledge. The data (Fig. 6) showed a small acceleration on the AO7 decolorization in the presence of 5.0 mg/L HA, the similar phenomenon was also displayed in the decomposition of PS. But AO7 and PS were not decomposed without ZVI, indicating that HA could not activate PS to produce $SO_4^{-\bullet}$. When HA decreased to 0.5 mg/L in the reaction solutions, the rate constants of AO7 decolorization increased from 0.048 to 0.101 min^{-1} (Table S6). However, HA showed a clearly deceleration on the AO7 decolorization when its concentration was greater than 5.0 mg/L. The rate constants in the presence of 1.0, 5.0, 7.5 and 10 mg/L of HA were 0.105, 0.049, 0.041 and 0.045 min^{-1}, respectively. Based on the results, we speculated that HA acted as an electron shuttle and the chelation of iron made its influence on AO7 decomposition very interesting. The concentrations of Fe^{2+} and total dissolved iron also increased dramatically in the presence of HA (5.0 mg/L) as compared to the control system without HA (Fig. 7). It was reported that primary functional groups including quinones, carboxylic acids, alcohols, and ketones in humic substances acted as soluble electron carriers to facilitate the degradation of pollutants by accepting electrons from ZVI and 'shuttling' the electrons to the H_2O_2 in Fenton reactions[43].Therefore, the presence of HA boosted the electron transfer from ZVI surface to the PS and resulted in the accelerating formation of Fe^{2+} and $SO_4^{-\bullet}$ in the PS/ZVI system.

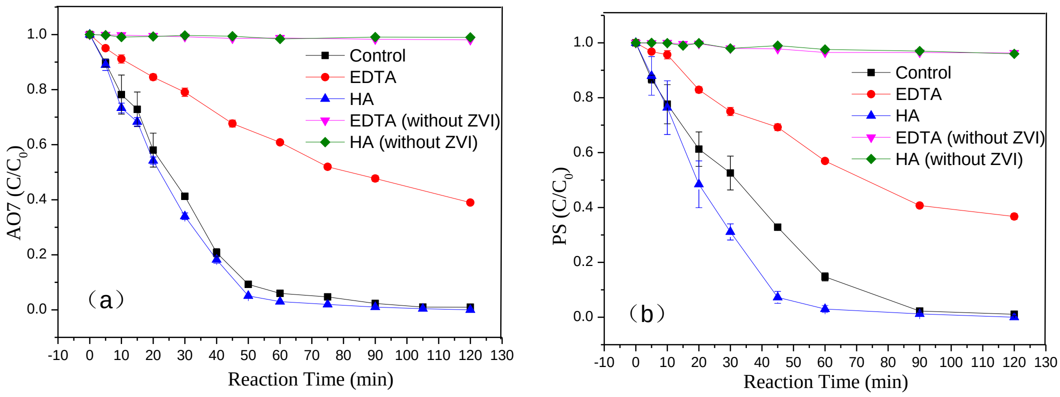

Fig. 6. (a). The effect of common organic matters on the decolorization of AO7; (b). The effect of common organic matters on the decomposition of PS. Experiment condition: PS = 2 mM; AO7 = 0.2 mM; ZVI = 0.5 g/L; EDTA = 50 mM; HA = 5.0 mg/L T = 25 °C.

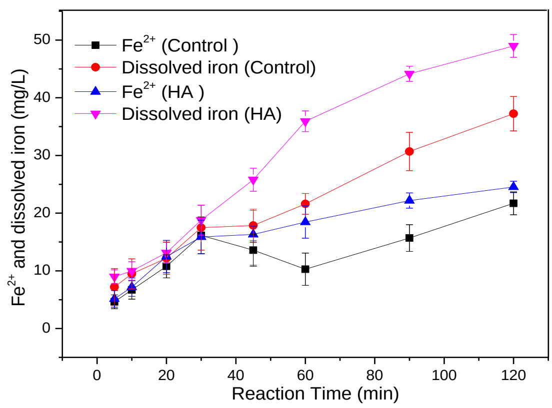

Fig. 7. The variation of iron ions in the presence and absence of HA versus reaction time. Experiment condition: PS = 2 mM; AO7 = 0.2 mM; ZVI = 0.5 g/L; HA = 5.0 mg/L; T = 25 °C.

3.5 Effect in simulated ground water

The decolorization of AO7 by activation of PS was studied in simulated ground water that contained a defined composition of inorganic and organic matter, including $Fe(NO_3)_3$ $9H_2O$ (0.24 μM), $NaHCO_3$ (1.2 mM), Na_2SO_4 (0.34 mM), Na_2HPO4 (0.28 mM), NaCl (0.86 mM) and catechol (1 ppm)[8,44]. As displayed in Fig. 8, the AO7 decolorization was significantly retarded in the simulated ground water compared to distilled water, especially in the first 60 min. After that, AO7 decolorized rapidly and reached 56.2% decolorization rate in 120 min. That was due to the scavenging reactions occurred between organic matters and $SO_4^{-\bullet}$. On the other hand, the initial pH was changed to 6.83 when these inorganic and organic matters were added into distilled water to prepare simulated ground water, which declined the AO7 decolorization rate based on the above discussion.

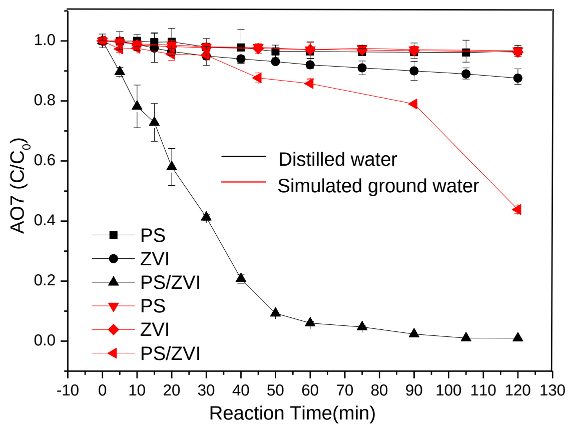

Fig. 8. Decolorization of AO7 in simulated ground water. Experiment condition: PS = 2 mM; AO7 = 0.2 mM; ZVI = 0.5 g/L; T = 25 °C.

4. Conclusions

It was demonstrated that maximum AO7 decolorization occurred at pH 3.0. Increasing system pH resulted in a greater decrease in AO7 decolorization rates. AO7 decolorization efficiency was 100% at 120 min when the molar ratio of PS:AO7 was 5:1. The overall oxidation rate of AO7 was effective upon addition of NO_3^-, NO_2^-, SO_4^{2-}, Cl^-, CO_3^{2-}, HCO_3^-, HPO_4^{2-}, $H_2PO_4^-$ and EDTA, whereas ClO_4^-, CH_3COO^- and HA were found to accelerate AO7 decolorization rates. ClO_4^-, CH_3COO^- and HA with 50 mM, 10 mM and 1.0 mg/L, respectively were found to be the optimal concentration for AO7 decolorization. The other inorganic ions also exhibited respective level of effect on decolorizing of AO7, which was ranged as NO_2^- > $H_2PO_4^-$ > HPO_4^{2-} > EDTA > SO_4^{2-} > CO_3^{2-} > HCO_3^- > NO_3^-> Cl^-. The removal efficiencies of AO7 were decreased by 90.3%, 51.5% and 58.7%, respectively over 120 min in addition of NO_2^- (50 mM), $H_2PO_4^-$ (50 mM) and HPO_4^{2-} (50 mM). While other inorganic ions including SO_4^{2-}, CO_3^{2-}, HCO_3^-, NO_3^-, Cl^- led to a decrease change of less than 20%.

On the basis of the above results and discussion, the reasons for the influence were as follows. (1) The ferric and ferrous ions underwent a complex reactions with $H_2PO_4^-$, HPO_4^{2-}, SO_4^{2-}, CO_3^{2-}, and HCO_3^-, causing ions precipitation (such as $H_2PO_4^-$ and HPO_4^{2-}) to lose the active iron to activate PS and affecting the distribution of iron species. (2) Scavenging reactions occurred between inorganic ions and $SO_4^{-\bullet}$ and formation of less reactive inorganic radicals (such as $HCO_3^{\cdot}$ and CO_3^{-}), which led to less $SO_4^{-\bullet}$ towards AO7. (3) Oxidation reactions involving inorganic ions (such as NO_2^-) consumed $SO_4^{-\bullet}$. The mechanism of the acceleration by CH_3COO^- and HA was probably through acting as an electron ‘shuttle’ and facilitating electron transfer from ZVI surface to PS, which led to more Fe^{2+} releasing to the PS/ZVI systems to some extent. Furthermore, Fe^{2+} was continued to release and activate PS effectively during the reaction time. These findings indicate that CH_3COO^- and HA played an important role in activated PS applications. It was speculated that the AO7 decolorization enhancement caused by ClO_4^- was presumably ascribed to the oxidizing of ZVI directly by ClO_4^-, which produced more Fe^{2+}. The other anions and organic matters have been shown to affect wastewater treatment processes involved $SO_4^{-\bullet}$. Activation of PS for degradation of refractory contaminants is a promising strategy in AOPs. The findings of this study will help achieve a deeper understanding of the impact of common inorganic ions and organic matters on the PS-based AOPs, which boosts the development of $SO_4^{-\bullet}$-based AOPs.

Acknowledgments

This research has been supported by National Natural Science Foundation of China (No. 51208206), Guangdong Provincial Department of Science (No. 2012A032300015), State Key Laboratory of Pulp and Paper Engineering in China (201213) and High-level Personnel Foundation of Guangdong Higher Education Institutions.

Appendix A. Supplementary material

Supplementary data associated with this article can be found, in the online version.

References

[1] Y. Peng, D. Fu, R. Liu, F. Zhang, X. Liang, $NaNO_2/FeCl_3$ catalyzed wet oxidation of the azo dye acid orange 7, Chemosphere 71 (2008) 990-997.

[2] A. Azam, A. Hamid, Effects of gap size and UV dosage on decolorization of C.I. acid orange 7 by UV/H_2O_2 process, J. Hazard. Mater. 133 (2006) 167-171.

[3] P. Neta, R. E Huie, A.B. Ross, Rate constants for reactions of inorganic radicals in aqueous solution, J. Phys. Chem. 17 (1998) 1027-1082.

[4] J.H. Ramírez, C.A. Costa, L.M. Madeira, G. Mata, M.A.Vicente, M.L. Rojas-Cervantes, A.J. López-Peinado, R.M. Martín-Aranda, Fenton-like oxidation of Orange II solutions using heterogeneous catalysts based on saponite clay, Appl. Catal., B. 71 (2007a) 44-56.

[5] H.J.H. Fenton, Oxidation of tartaric acid in presence of iron, J. Chem. Soc. 65 (1894) 899-910.

[6] C. Cuypers, T. Grotenhuis, J. Joziasse, W. Rulkens, Rapid persulfate oxidation predicts PAH bioavailability in soils and sediments, Environ. Sci. Technol. 34 (2000) 2057-2063.

[7] P.H. Shi, R.J. Su, F.Z. Wan, M.C. Zhu, D.X. Li, S.H. Xu, Co_3O_4 nanocrystals on graphene oxide as a synergistic catalyst for degradation of Orange II in water by advanced oxidation technology based on sulfate radicals. Appl. Catal., B. 123-124 (2012) 265-272.

[8] S. Gokulakrishnan, P. Parakh, H. Prakash, Photodegradation of methyl orange and photoinactivation of bacteria by visible light activation of persulphate using a tris(2,2'-bipyridyl)ruthenium(II) complex, Photochem. Photobiol. Sci. 12 (2013) 456-66.

[9] M.G. Antoniou, A.A. de la Cruz, D.D. Dionysiou, Degradation of microcystin-LR using sulfate radicals generated through photolysis, thermolysis and e^- transfer mechanisms, Appl. Catal., B. 96 (2010) 290-298.

[10] S. Bougie, J.S. Dube, Oxidation of dichlorobenzene isomers with the help of thermally activated sodium persulfate, J. Environ. Eng. Sci. 6 (2007) 397-407.

[11] S. Ahn, T. D. Peterson, J. Righter, D. M. Miles and P. G. Tratnyek, Disinfection of Ballast Water with Iron Activated Persulfate. Environ. Sci. Technol. 47(2013) 11717-11725.

[12] S. Gokulakrishnan, P. Parakh, H. Prakash, Degradation of Malachite green by Potassium persulphate, its enhancement by 1,8-dimethyl-1,3,6,8,10,13-hexaazacyclotetradecane nickel(II) perchlorate complex, and removal of antibacterial activityJ. Hazard. Mater. 213-214 (2012) 19-27.

[13] S. Gokulakrishnan, N. Pranav, S.J. Hinder, S.C. Pillai, H. Prakash, Nickel azamacrocyclic complex activated persulphate based oxidative degradation of methyl orange: recovery and reuse of complex using adsorbents RSC Adv. 5 (2015) 31716-31724.

[14] H.X. Li, J.Q.Wan, Y.W. Ma, Y. Wang, Y.M. Chen, New insights into the role of zero-valent iron surface oxidation layers in persulfate oxidation of dibutyl phthalate solutions, Chem. Eng. J. 237 (2014) 487-496.

[15] H.X. Li, J.Q. Wan, Y.W. Ma, Y. Wang, M.Z. Huang, Influence of particle size of zero-valent iron and dissolved silica on the reactivity of activated persulfate for degradation of acid orange 7, Chem. Eng. J. 237 (2014) 487-496.

[16] X.G. Gu, S.G. Lu, X.H. Guo, J.K. Sima, Z.F. Qiua, Q. Suia , Oxidation and reduction performance of 1,1,1-trichloroethane in aqueous solution by means of a combination of persulfate and zero-valent iron, RSC Adv. 5 (2015) 60849-60856.

[17] H.Q. Sun, G.L. Zhou, S.Z. Liu, H.M. Ang, M.O. Tadé, S.B. Wang, Nano-Fe^0 encapsulated in carbon spheres for oxidation of aqueous phenol with sulphate radicals, ACS-Appl. Mater. Interface. 4 (2012) 6235-6241.

[18] L. De Laat, G.T. Le, B. Legube, A comparative study of the effects of chloride, sulfate and nitrate ions on the rates of decomposition of H_2O_2 and organic compounds by Fe(II)/H_2O_2 and Fe(III), Chemosphere 55 (2004) 715-723.

[19] E.M. Siedlecka, A. Wieckowska, P. Stepnowski, Influence of inorganic ions on MTBE degradation by Fenton's reagent, J. Hazard. Mater. 147 (2007) 497-502.

[20] L.R. Bennedsen, J. Muff, E.G. Søgaard, Influence of chloride and carbonates on the reactivity of activated persulfate, Chemosphere 86 (2012) 1092-1097.

[21] L. De Laat, G.T. Le, Effects of chloride ions on the iron(III)-catalyzed decomposition of hydrogen peroxide and on the efficiency of the Fenton-like oxidation process, Appl. Catal., B. 66 (2006) 137-146.

[22] F.J. Beltran, M. Gonzalez, F.J. Rivas, P. Alvarez, Fenton reagent advanced oxidation of polynuclear aromatic hydrocarbons in water, Water Air Soil Pollut. 105 (1998) 685-700.

[23] C.J. Liang, Z. Wang, N. Mohanty, Influences of carbonate and chloride ions on persulfate

oxidation of trichloroethylene at 20 ℃, Environ. Sci. Technol. 370 (2006): 271-277.

[24] K.C. Huang, R.A. Couttenye, G.E. Hoag, Kinetics of heat-assisted persulfate oxidation of methyl tert-butyl ether (MTBE), Chemosphere 49 (2002) 413-420.

[25] S.Y. Yang, P. Wang, X. Yang, L. Shan, W.Y. Zhang, X.T. Shao, R. Niu, Degradation efficiencies of azo dye Acid Orange 7 by the interaction of heat, UV and anions with common oxidants: Persulfate, peroxymonosulfate and hydrogen peroxide, J. Hazard. Mater. 179 (2010) 552-558

[26] X.R. Xu, X.Z. Li, Degradation of azo dye Orange G in aqueous solutions by persulfate with ferrous ion, Sep. Purif. Technol. 72 (2010) 105-111.

[27] S. Y. Yang, X. Yang, X.T. Shao, R. Niu, L. L. Wang, Activated carbon catalyzed persulfate oxidation of Azo dye acid orange 7 at ambient temperature, J. Hazar. Mater. 186 (2011) 659-666.

[28] G.P. Anipsitakis, D.D. Dionysiou, Radical generation by the interaction of transition metals with common oxidants, Environ. Sci. Technol. 38 (2004) 3705-3712.

[29] C. Liang, C.F. Huang, N. Mohanty, R.M. Kurakalva, A rapid spectrophotometric determination of persulfate anion in ISCO, Chemosphere 73 (2008) 1540-1543.

[30] APHA, AWWA, WEF, Standards Methods for the Examination of Water and Wastewater, APHA, Washington, DC, 1998.

[31] M. Kumar, S. Chakraborty, Chemical denitrification of water by zero-valent magnesium powder. J. Hazard. Mater. 135 (2006) 112-121.

[32] J. J. Pignatello, E. Oliveros, A. MacKay, Advanced Oxidation Processes for Organic Contaminant Destruction Based on the Fenton Reaction and Related Chemistry, Critical Reviews in Environ. Sci. Technol. 36 (2007) 1-84.

[33] G.V. Buxton, C.L. Greenstock, W.P. Helman, A.B. Ross, Critical review of rate constants for reactions of hydrated electrons, hydrogen atoms and hydroxyl radicals ($\cdot OH/\cdot O^-$)in aqueous solutions, J. Phys. Chem. Ref. 17 (1988) 513-886.

[34] E. Lipczynska-Kochany, G. Sprah, S. Harms, Influence of some groundwater and surface waters constituents on the degradation of 4-chlorophenol by the Fenton reaction, Chemosphere 30 (1995) 9-20.

[35] X.Y. Yu, Z.C. Bao, J.R. Barker, Free radical reactions involving Cl, Cl_2^-, and SO_4^- in the 248 nm photolysis of aqueous solutions containing $S_2O_8^{2-}$and Cl^-, J. Phys. Chem. A. 108 (2004) 295-308.

[36] G. Le Truong, J. De Laat, B. Legube, Effects of chloride and sulfate on the rate of oxidation of ferrous ion by H_2O_2. Water. Res. 38 (2004) 2384-2394.

[37] D.W. King, R. Farlow, Role of carbonate speciation on the oxidation of Fe II by H_2O_2, Mar. Chem. 70 (2000) 201-209.

[38] C.M. Miller, Hydrogen Peroxide Decomposition and Contaminant Degradation in the Presence of Sandy Aquifer Materials. Dissertation, The University of Iowa. 1995.

[39] Z. Zuo, Z. Cai, Y. Katsumura, N. Chitose, Y. Muroya, Reinvestigation of the acid-base equilibrium of the (bi)carbonate radical and pH dependence of its reactivity with inorganic reactants, Radiat Phys Chem 55 (1999)15-23.

[40] T.P. Knepper, Synthetic chelating agents and compounds exhibiting complexing properties in the aquatic environment. TrAC – Trends Anal. Chem. 22 (2003) 708-724.

[41] C.J Liang, C.J. Bruell, M.C. Marley, K.L Sperry, Persulfate oxidation for in situ remediation of TCE. II. Activated by chelated ferrous ion, Chemosphere 55 (2004) 1225-1233.

[42] C.G. Niu, Y. Wang, X.G. Zhang, G.M. Zeng, D.W. Huang, M. Ruan, X.W. Li, Decolorization of an azo dye Orange G in microbial fuel cells using Fe(II)-EDTAcatalyzed persulfate, Bioresour. Technol. 126 (2012) 101-106.

[43] S. H. Kang, W. Y. Choi, Oxidative Degradation of Organic Compounds Using Zero-Valent Iron in the Presence of Natural Organic Matter Serving as an Electron Shuttle. Environ. Sci. Technol. 43 (2009)878-883.

[44] J. Marugan, R. V. Grieken, C. Pablos and C. Sordo, Analogies and differences between photocatalytic oxidation of chemicals and photocatalytic inactivation of microorganisms, Water Res., 44 (2010) 789-796.

Graphical Abstract